

## Electrical transport in magnetite near the Verwey transition

A. J. M. Kuipers and V. A. M. Brabers

*Department of Physics, Eindhoven University of Technology, Eindhoven, The Netherlands*

(Received 19 January 1979)

Thermoelectric power and conductivity measurements were carried out on Ti-doped single crystals of magnetite in the temperature range 70–300 K. The analysis of the measurements supports the model in which the electrical conduction below the Verwey transition takes place on two energy levels separated by a gap of about 0.12 eV. Evidence is found that the mobility of the electrons is thermally activated above as well as below the Verwey transition, indicating phonon-assisted tunneling.

### I. INTRODUCTION

At about 120 K magnetite ( $\text{Fe}_3\text{O}_4$ ) exhibits the well-known Verwey transition. At the Verwey temperature ( $T_V$ ), the transition is induced by an ordering of the electrons on the octahedral iron sites in the low-temperature phase. The electrical conduction in this temperature region has been for years a quite intricate problem. Electrical conductivity, thermoelectric power, and Hall-effect measurements which have been performed were not able to elucidate satisfactorily the electrical transport mechanism. For instance the sign of the charge carriers could not unambiguously be established. (For an extensive literature survey see Ref. 1.)

Recently, a model has been suggested<sup>1</sup> for describing the transport properties. The model is based upon measurements of the thermoelectric power on nearly stoichiometric magnetite single crystals. It appeared that minor deviations from stoichiometry had a decisive influence whether *p*- or *n*-type conduction was observed in the ordered state. To explain these results, we proposed a model by which the conduction below the Verwey transition takes place by charge transport in two energy levels which are separated by an energy gap of about 0.1 eV. This gap should arise from the electron ordering. Within this model it is also possible that a small amount of impurities, which produce a change of the  $\text{Fe}^{2+}$  to  $\text{Fe}^{3+}$  ratio, will establish a change of sign of the majority charge carriers. For that purpose titanium is a suitable substitution, since—substituted in magnetite—it has always the valency 4<sup>+</sup>. In order to check experimentally the proposed model and to get more quantitative information above the various parameters involved, we performed measurements of thermoelectric power and conductivity on titanium-doped single crystals of magnetite. Moreover from a combined analysis of these data we were able to deduce the behavior of the mobility of the charge carriers in the

low-temperature phase of magnetite.

### II. EXPERIMENTAL

Synthetic single crystals of Ti-doped magnetite were prepared from  $\text{Fe}_2\text{O}_3$  and  $\text{TiO}_2$  by means of a floating-zone technique in an arc-image furnace<sup>2</sup>; six different compositions were prepared with  $x = 0$ ,  $10^{-4}$ ,  $4 \times 10^{-4}$ ,  $10^{-3}$ ,  $3 \times 10^{-3}$ , and  $8 \times 10^{-3}$ , (see definition of  $x$  in Sec. III) respectively. After the crystallization the samples were annealed for 70 h at 1130 °C in a  $\text{CO}_2$ - $\text{H}_2$  mixture with a partial oxygen pressure of  $10^{-10}$  atm. During cooling to room temperature the  $\text{CO}_2$ - $\text{H}_2$  ratio was changed in such a way that the curve, representing the partial oxygen pressure as function of the inverse temperature, was parallel to the curve representing the  $\text{Fe}_3\text{O}_4$ - $\text{FeO}$  phase boundary. Such a procedure was previously proposed by Smiltens to obtain stoichiometric magnetite crystals.<sup>3</sup> In the specimens obtained no phase segregation was observed either with x ray or with microscopic investigations.

To prevent the inclusion of undesirable impurities, the iron(III) oxide used as starting material was prepared from electrolytical iron dissolved in HCl. From this solution iron(II) oxalate was precipitated by means of oxalic acid. By firing in the air the iron oxalate decomposes into iron(III) oxide. The iron(III) oxide prepared in this way has a purity of 99.9999% as far as metal impurities are concerned.

In the temperature range 70–240 K thermoelectric power and conductivity measurements were performed on cylindrical crystals with typical dimensions of 3 cm length and 0.5 cm diameter. The [110] direction was parallel to the axis of the samples. Since no precautions were taken to prevent twinning below  $T_V$ , all the measurements in this temperature region were carried out on twinned specimens. Details of the measuring procedure have been published previously.<sup>1</sup>

### III. TWO-LEVEL MODEL

In the two-level model for the electrical conduction of magnetite below the Verwey transition, it is supposed that the  $3d^6$  electron states of the octahedral iron ions are divided into two sets of energy levels, equal in number and separated by an energy gap of  $2\Delta$ . Since in a stoichiometric specimen of magnetite the number of  $\text{Fe}^{2+}$  ions equals half the number of octahedral sites this implies that in such a specimen at  $T=0$  the states below the gap are completely filled with electrons, whereas the states above the gap are empty. Charge carriers either are created by excitations of electrons across the gap at  $T \neq 0$  or are introduced by mono- and tetra-valent metal impurities and oxygen nonstoichiometry.

If the zero of the energy scale is chosen in the middle of the gap, the distribution of the electrons between the two energy levels is according to Fermi-Dirac statistics given by

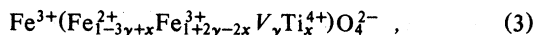
$$n_1 = \frac{N_0}{1 + \exp\{(-\Delta - E_F)/kT\}} \quad (1a)$$

$$n_2 = \frac{N_0}{1 + \exp\{(\Delta - E_F)/kT\}} \quad (1b)$$

In these equations  $n_1$  and  $n_2$  are the numbers of electrons per unit volume below and above the energy gap, respectively.  $N_0$  is the number of available sites in each level, which equals half the number of octahedral sites. In stoichiometric magnetite  $N_0 = N$ , where  $N$  is the number of formula units per unit volume. The number of negative charge carriers  $n$  equals  $n_2$ , whereas the number of positive charge carriers is given by  $p = N_0 - n_1$ . If we denote the total number of electrons by  $n_t$  (for stoichiometric magnetite  $n_t = N$ ), the Fermi energy can be calculated from the equation

$$n_1 + n_2 = n_t \quad (2)$$

If we write the formula for nonstoichiometric magnetite (characterized by the octahedral vacancy concentration  $\gamma$ ) doped with an amount of  $x$  Ti ions per formula unit as



then the total number of electrons is given by  $n_t = N(1 - 3\gamma + x)$  and the number of states in each level equals  $N_0 = N(1 - \frac{1}{2}\gamma - \frac{1}{2}x)$ .

The Seebeck coefficient within this model can be written

$$S = \frac{1}{eT} \frac{-n(\Delta - E_F) + p(\Delta + E_F)\mu_p/\mu_n}{n + p\mu_p/\mu_n} \quad (4)$$

In expression (4) the terms due to transport of kinetic energy are omitted. This may be justified by the fact that in narrow bands these terms are generally

expected to be small and probably zero in the case of hopping conduction.<sup>4</sup>

In Eq. (4)  $\mu_p$  and  $\mu_n$  are the mobilities of the  $p$ - and  $n$ -type charge carriers, respectively. These mobilities may quite generally be written

$$\mu_p = \mu_{0,p}(T)e^{-q_p/kT} \quad (5a)$$

$$\mu_n = \mu_{0,n}(T)e^{-q_n/kT} \quad (5b)$$

where the activation energies  $q_p$  and  $q_n$  are not necessarily different from zero and  $\mu_{0,p}$  and  $\mu_{0,n}$  depend on  $T$  by some power law. The quotient  $\mu_p/\mu_n$  can be given by

$$\frac{\mu_p}{\mu_n} = f(T)e^{-\Delta q/kT} \quad (6)$$

From this equation we can find two limiting cases, viz,

$$\frac{\mu_p}{\mu_n} = e^{-\Delta q/kT} \quad (7)$$

and

$$\frac{\mu_p}{\mu_n} = c \quad (8)$$

where  $c$  is a constant of order unity.

Both cases will be considered for the interpretation of our measurements in Sec. IV.

### IV. RESULTS AND DISCUSSION

The absolute thermoelectric power,<sup>5</sup> measured on six samples with different compositions, is plotted versus temperature in Fig. 1. Except for the specimen with the largest Ti concentration ( $x = 8 \times 10^{-3}$ ) the values of the Seebeck coefficient above the Verwey transition are equal within experimental error and are also in agreement with previous results.<sup>1</sup> At the Verwey transition a sharp decrease of the Seebeck coefficient is observed for all specimens and in the ordered state the influence of the titanium dope is rather pronounced. When the temperature is lowered further below  $T_V$ , the specimens with  $x = 0$  and  $x = 10^{-4}$  reveal a marked rise of the Seebeck coefficient, reaching a value of about  $+250 \mu\text{V/K}$  at 70 K. This behavior is analogous to that of the nearly stoichiometric specimens described previously.<sup>1</sup> With decreasing temperature the thermoelectric power of the sample with  $x = 4 \times 10^{-4}$  increases until  $T = 85 \text{ K}$  and then decreases. The specimens with  $x > 4 \times 10^{-4}$  all show a sudden drop of the Seebeck coefficient below  $T_V$  with a value of about  $-500 \mu\text{V/K}$  at 70 K.

If we take the two-level model of Sec. III for the interpretation of the Seebeck measurements, the number of electrons ( $\text{Fe}^{2+}$  ions) in relation to the

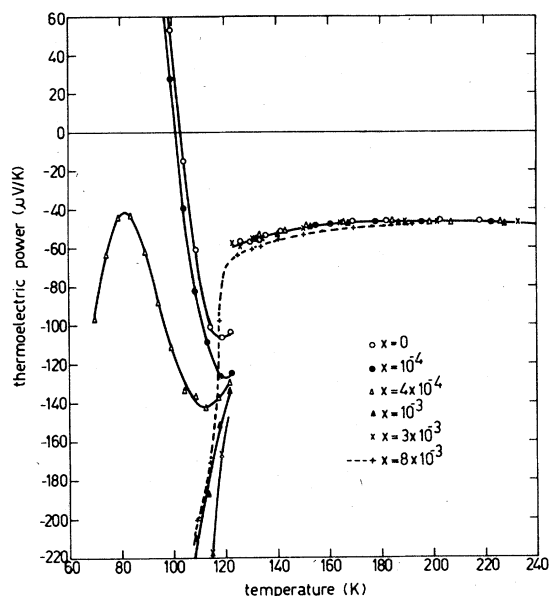


FIG. 1. Absolute thermoelectric power of  $\text{Fe}_{3-x}\text{Ti}_x\text{O}_4$  vs temperature.

number of available states in the lowest level is then decisive whether  $p$ - or  $n$ -type conduction at  $T=0$  can be expected; that means that stoichiometry and impurity content determine the sign of the thermopower.

Since the magnetite specimens were annealed under the same experimental conditions, the vacancy concentration  $\gamma$  may be supposed to be constant and as titanium is the main impurity in our samples, we can expect according to the model, a sign reversal of the thermopower at  $T=0$  for a composition  $x$ , when  $1 - 3\gamma + x = 1 - \frac{1}{2}\gamma - \frac{1}{2}x$ , that means  $x = \frac{5}{3}\gamma$ . The fact that in the experimental data at low temperatures a sign reversal occurs between  $x = 10^{-4}$  and  $x = 4 \times 10^{-4}$  implies that, within this model, the possible values of  $\gamma$  are restricted to  $6 \times 10^{-5} < \gamma < 2.4 \times 10^{-4}$ .

We calculated the Seebeck coefficients for various values of  $\gamma$  within this range from the Eqs. (1)–(4) and (7). A typical example with  $\gamma = 2 \times 10^{-4}$ ,  $2\Delta = 0.134$  eV, and  $\Delta q = 0.007$  eV has been plotted in Fig. 2(a). However, it appeared that for all specimens—except for  $x = 4 \times 10^{-4}$  at low temperatures—a better agreement is obtained with a value of  $\gamma$  larger than  $2.4 \times 10^{-4}$ . An example with

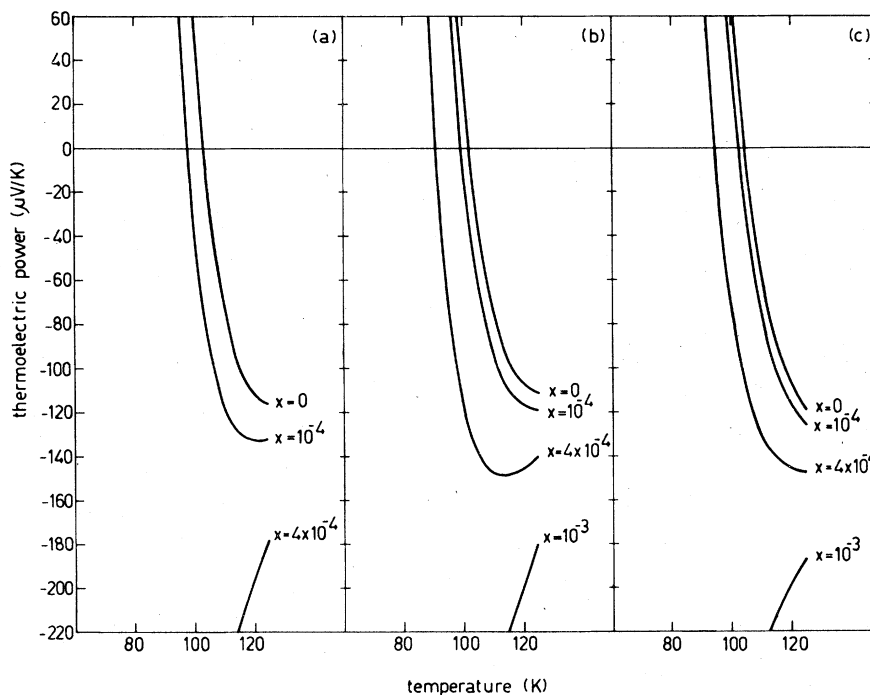


FIG. 2. Temperature dependence of the Seebeck coefficient calculated according to the model outlined in Sec. III with the titanium concentration  $x$  as parameter. (a)  $\gamma = 2 \times 10^{-4}$ ,  $2\Delta = 0.134$  eV,  $\mu_p/\mu_n$  according to Eq. (7) with  $\Delta q = 0.0070$  eV; (b)  $\gamma = 4.7 \times 10^{-4}$ ,  $2\Delta = 0.120$  eV,  $\mu_p/\mu_n$  according to Eq. (7) with  $\Delta q = 0.0078$  eV; (c)  $\gamma = 4.7 \times 10^{-4}$ ,  $2\Delta = 0.120$  eV,  $\mu_p/\mu_n$  according to Eq. (8) with  $c = 0.47$ .

$\gamma = 4.7 \times 10^{-4}$ ,  $2\Delta = 0.120$  eV, and  $\Delta q = 0.0078$  eV is shown in Fig. 2(b). For comparison we have plotted in Fig. 2(c) the Seebeck coefficient calculated with the same values of the parameters  $\Delta$  and  $\gamma$  but using expression (8) instead of Eq. (7) for  $\mu_p/\mu_n$  with  $c = 0.47$ . It is emphasized that the parameter values which were used for these plots do not necessarily give the best agreement; the plots are principally meant as an example. However, deviations from these values larger than about 10% appeared in all

cases to deteriorate significantly the correspondence with the experimental results. The thermoelectric power of Ti-substituted magnetite in the temperature range of 90–120 K can be well predicted quantitatively by our two-level model approximation, but below 90 K the experimental results deviate widely from the calculations, particularly for the sample  $x = 4 \times 10^{-4}$ . As the  $\text{Fe}^{2+}$  to  $\text{Fe}^{3+}$  ratio in the specimens plays a decisive role for the thermoelectric power in the low-temperature phase, it is obvious that a complex tem-

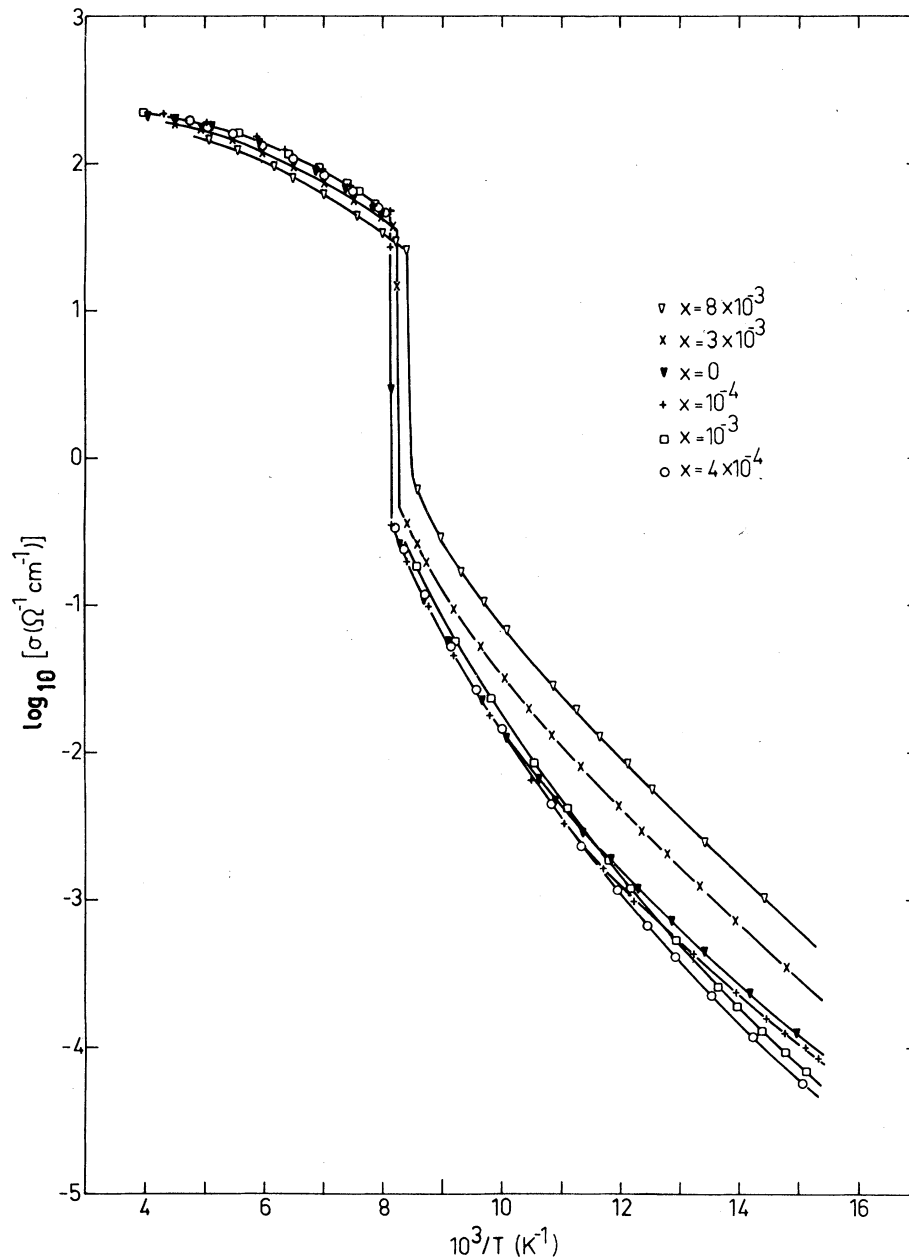


FIG. 3. Logarithm of the conductivity of  $\text{Fe}_{3-x}\text{Ti}_x\text{O}_4$  vs reciprocal temperature.

perature dependence can be expected if impurities which create or destroy  $\text{Fe}^{2+}$  ions, i.e.,  $\text{Ti}^{4+}$  ions and cation vacancies, are present in nearly equal concentrations. In our opinion the origin of the anomalous behavior below 90 K can be found in the interactions of the charge carriers with these titanium ions and cation vacancies. It can be argued that a  $\text{Ti}^{4+}$  ion will lower the energy levels of neighboring iron sites.<sup>6</sup> The implication of this lowering of the site energies upon the electrical conduction may be described in two ways. From the first point of view, one can regard the respective sites as electron traps and consequently consider the combination  $\text{Fe}^{2+}\text{-Ti}^{4+}$  as a donor.

On the other hand, in the case of hopping conduction, the lowering of a part of the site energies may be considered to decrease the electron mobility, since an electron on such a site will need a larger activation energy to make a transition to another site. If conduction takes place by hopping it is hard to discriminate between the two descriptions, which is also the problem in the theory of electrical conduction in disordered systems.<sup>7</sup> However, the descriptions are equivalent in so far as both yield a decrease of the conductivity of the  $n$ -type charge carriers ( $\sigma_n$ ) in presence of  $\text{Ti}^{4+}$  ions. In a similar way a vacancy, which is negatively charged relative to a  $\text{Fe}^{3+}$  ion will lower the conductivity of the  $p$ -type charge carriers ( $\sigma_p$ ), because the combination  $V\text{-Fe}^{3+}$  acts as an acceptor.

Since for the specimen  $x = 4 \times 10^{-4}$ ,  $\sigma_n$  and  $\sigma_p$  are almost equal, small variations of the energy levels, caused by Ti ions and vacancies, will have a complex impact on the temperature dependence of the thermoelectric power. The two-level model we used, explains best the data of the thermopower just below  $T_V$  in the case that there are majority charge carriers.

The electrical conductivity of the crystals used for the thermoelectric power measurements was also determined as function of temperature. In Fig. 3 the results of these measurements are represented. Except for the samples with  $x = 3 \times 10^{-3}$  and  $x = 8 \times 10^{-3}$  the values above  $T_V$  are equal within experimental error. Below  $T_V$  the values of the conductivity slightly diverge with decreasing temperature, the conductivity of the sample with  $x = 4 \times 10^{-4}$  being lowest. In contrast to the low-temperature phase, where the conductivities of the samples with  $x = 3 \times 10^{-3}$  and  $x = 8 \times 10^{-3}$  are larger than those of the four purest specimens, above  $T_V$  the conductivity of the two most impure specimens is smaller compared with the more pure samples. The transition temperature of the latter four specimens is equal within experimental error and equals 123.1 K. In the samples with  $x = 3 \times 10^{-3}$  and  $x = 8 \times 10^{-3}$  the transition takes place at 121.2 and 118.6 K, respectively.

Qualitatively, these results are in agreement with the behavior reported in literature.<sup>8</sup> With the two-

level model it is now possible to calculate the conductivity of the Ti-doped magnetites using the formula

$$\sigma = ne\mu_n + pe\mu_p = Ne\mu_n \left( \frac{n}{N} + \frac{p}{N} \frac{\mu_p}{\mu_n} \right) \quad (9)$$

$N$  is the number of electrons per  $\text{cm}^3$  for stoichiometric magnetite, i.e., the number of  $\text{Fe}^{2+}$  ions. The expression within the brackets can be calculated using some parameters already determined from thermopower measurements. As an example, the logarithm of this expression, calculated with the parameter values of Fig. 2(c), is plotted in Fig. 4. By combining these calculated data with the experimental results of the conductivity measurements presented in Fig. 3, we obtain the value of  $Ne\mu_n$ . In Fig. 5 we have plotted the resulting values of  $Ne\mu_n$  which were calculated from the data of the samples with  $x = 0$  to  $x = 10^{-3}$ . The error bars denote the range of values which are obtained from the set of conductivity data of these four samples at a certain temperature. A striking result of this analysis is the smooth join of the calculated value of  $Ne\mu_n$  in the low-temperature phase with the value of  $\sigma$  above  $T_V$  (cf. Fig. 5). In the high-temperature phase, the number of electrons, which equals the number of  $\text{Fe}^{2+}$  ions, is for all the Ti-doped specimens nearly constant and equal to  $N$ . If above  $T_V$ , where the energy gap has disappeared, all the electrons take part in the conduction process, Fig. 5 suggests that the nature of the jump in the conductivity is a change of the number of charge carriers and not a sudden change of the mobility. Within the analysis we propose here, it turns out that above as well as below the Verwey transition the mobility of the electrons is thermally activated, indicating that conduction takes place by

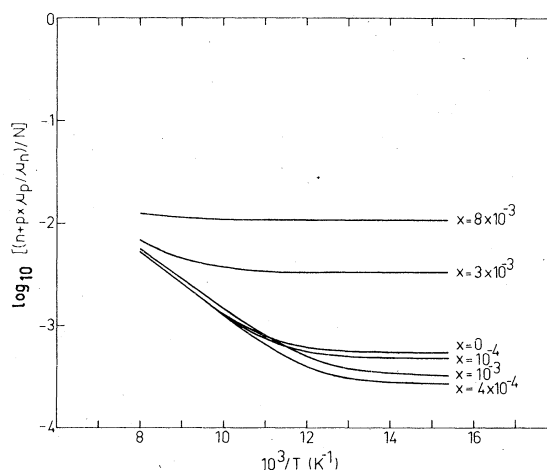


FIG. 4. Calculated values of  $\log_{10}[(n+p \times \mu_p/\mu_n)/N]$  with  $\gamma = 4.7 \times 10^{-4}$ ,  $2\Delta = 0.120$  eV, and  $\mu_p/\mu_n$  according to Eq. (8) with  $c = 0.47$ .

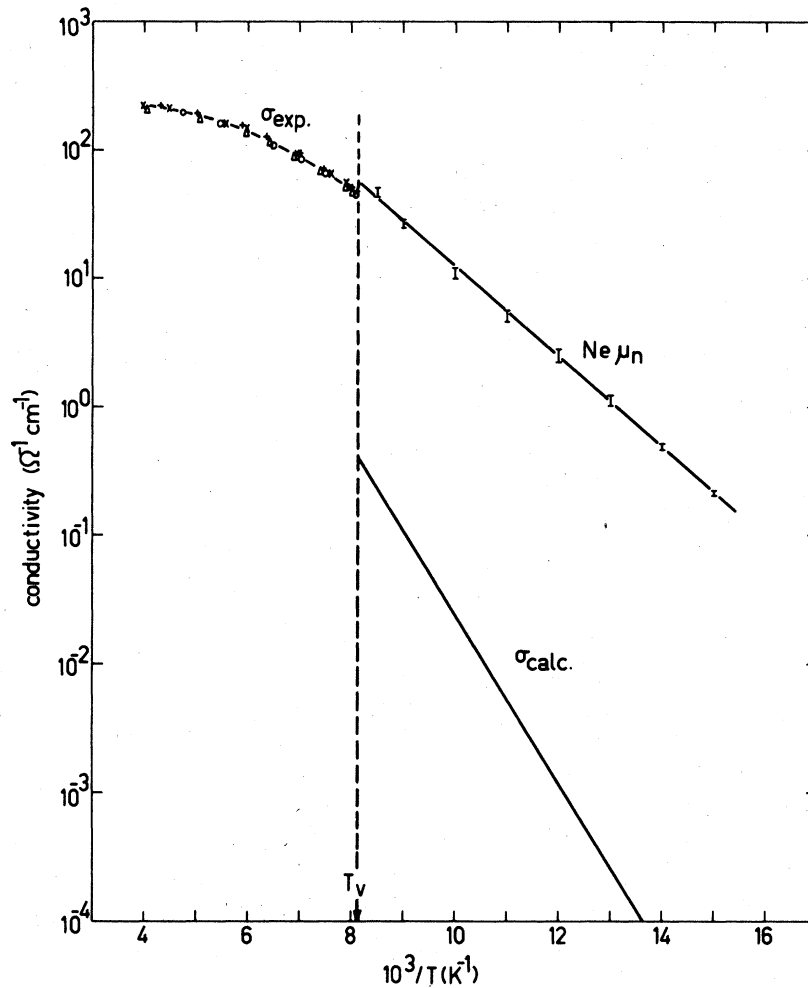


FIG. 5. Conductivity vs reciprocal temperature. The data points above  $T_V$  are the experimental results on the samples with  $x=0$  to  $x=10^{-3}$ . The error bars through the curve marked " $Ne\mu_n$ " represent the values of  $Ne\mu_n$  calculated according to formula (9) from the experimental values of Fig. 3 and the calculated results of Fig. 4 of the specimens with  $x=0$  to  $x=10^{-3}$ . The straight line marked " $\sigma_{calc.}$ " represents the value of the conductivity calculated with formula (9) using the drawn curve for  $Ne\mu_n$  and with  $x=0$ ,  $\gamma=0$ ,  $\mu_p/\mu_n=1$ , and  $2\Delta=0.120$  eV.

phonon-assisted tunneling (hopping). This analysis implies further than the origin of the thermally activated behavior of the mobility above and below the Verwey transition is similar. In that case the activated behavior above  $T_V$  cannot be related to the dynamic disorder of the electrons, as has been suggested by Klinger,<sup>9</sup> since below  $T_V$  there is no disorder.

It corroborates the idea that the origin of the activated behavior may be found in small polaron formation.

The values of  $Ne\mu_n$  determined from the conductivity measurements on samples  $x=3 \times 10^{-3}$  and  $x=8 \times 10^{-3}$  were slightly smaller than the values indicated in Fig. 5. However, in the model calculations we did not explicitly take into account the donor and

acceptor character of  $Ti^{4+}$  ions and metal vacancies, respectively. The decrease of  $\sigma_n$ , caused by the presence of Ti ions as mentioned before in the discussion on the thermopower, can also explain why the obtained values of  $Ne\mu_n$  for samples with large Ti concentrations are somewhat lower than predicted by our model. From the  $Ne\mu_n$  vs  $1/T$  plot in Fig. 5, a thermally activated mobility can be deduced, with an activation energy of 0.07 eV and a value of  $\mu_n$  at 120 K of about  $0.02$  cm<sup>2</sup>/Vsec. The conductivity of pure stoichiometric magnetite can also be calculated for the low-temperature phase using the plotted values of  $Ne\mu_n$ , the gap width  $2\Delta=0.12$  eV and the ratio  $\mu_p/\mu_n=1$ ; the result is presented in Fig. 5 by the line marked " $\sigma_{calc.}$ ".

If the interpretation of the measurements as out-

lined before is correct, several theoretical explanations of the conduction in magnetite have to be discarded. First there are those theories which do not predict an energy gap and the related creation of charge carriers below  $T_v$ . The model of Rosencwaig<sup>10</sup> and the theory of Camphausen and Chakraverty<sup>11</sup> belong to this category. Second, there are those theories, which in the low-temperature phase yield band conduction such as the Cullen and Callen model<sup>12</sup> and the theory of Buchenau.<sup>13</sup> In that case the mobility of the charge carriers would be constant or only weakly depending on the temperature, which is in contradiction with our results. As for the theory of Chakraverty<sup>14</sup> which explains the Verwey

transition on the basis of a Jahn-Teller distortion, it is hard to judge, because it is not clear how the conduction is explained within this model.

The most important conclusion, drawn from the present results is that the basic features of a two-level model describing the electrical conduction are applicable to the low-temperature phase of magnetite; an energy gap of about 0.12 eV exists between the two kinds of states. From the combined analysis of thermoelectric power and conductivity measurements, evidence is found that below as well as above the Verwey transition a thermal activated mobility of the electrons is found, indicating hopping conduction in both phases.

<sup>1</sup>A. J. M. Kuipers and V. A. M. Brabers, *Phys. Rev. B* **14**, 1401 (1976).

<sup>2</sup>C. Kooy and H. J. N. Couwenberg, *Philips Tech. Rev.* **23**, 161 (1962).

<sup>3</sup>J. Smiltens, *J. Chem. Phys.* **20**, 990 (1952).

<sup>4</sup>I. G. Austin and N. F. Mott, *Adv. Phys.* **18**, 41 (1969).

<sup>5</sup>Preliminary results of the thermoelectric power measurements have been presented at the Second International Conference on Ferrites, Paris, 1976; see A. J. M. Kuipers and V. A. M. Brabers, *J. Phys. (Paris)* **38**, C1-233 (1977).

<sup>6</sup>T. G. W. Stijntjes, J. Klerk, and A. Broese Van Groenou, *Philips Res. Rep.* **25**, 95 (1970); V. A. M. Brabers, *Appl. Phys.* **9**, 347 (1976); D. Ihle and B. Lorenz, *J. Phys. C* **10**, 1473 (1977).

<sup>7</sup>N. F. Mott and E. A. Davis, *Electronic Processes in Non-Crystalline Materials* (Clarendon, Oxford, 1971).

<sup>8</sup>E. J. W. Verwey, P. W. Haayman, *Physica (Utrecht)* **8**, 879 (1941); Y. Miyahara, *J. Phys. Soc. Jpn.* **32**, 629 (1971).

<sup>9</sup>M. I. Klinger, *J. Phys. C* **8**, 3595 (1975); M. I. Klinger and A. A. Samokhvalov, *Phys. Status Solidi B* **79**, 9 (1977).

<sup>10</sup>A. Rosencwaig, *Phys. Rev.* **181**, 946 (1969); *Can. J. Phys.* **47**, 2309 (1969).

<sup>11</sup>D. L. Camphausen and B. K. Chakraverty, in *Proceedings of the Eleventh International Conference on Semiconductors* (Polish Scientific, Warsaw, 1972), p. 1266.

<sup>12</sup>J. R. Cullen and E. Callen, *J. Appl. Phys.* **41**, 879 (1970); *Phys. Rev. Lett.* **26**, 236 (1971); *Phys. Rev. B* **7**, 397 (1973).

<sup>13</sup>U. Buchenau, *Solid State Commun.* **11**, 1287 (1972); *Phys. Status Solidi B* **70**, 181 (1975); U. Buchenau and I. Müller, *Physica (Utrecht) B* **80**, 75 (1975).

<sup>14</sup>B. K. Chakraverty, *Solid State Commun.* **15**, 1271 (1974).